Effect of Friction Time on the Mechanical and Microstructural Properties of AA6061 Joints by Continuous Drive Friction Welding

Mohammed A. Tashkandi
Mechanical Engineering Department
College of Engineering
Northern Border University
Arar, Saudi Arabia
tashkandi@gmail.com

Masoud Ibrahim Mohamed
Chemical Engineering and Material Science Dept., Faculty of Engineering, Northern Border University, Saudi Arabia
On leave from Mechanical Engineering Dept., Fayoum University, Egypt
ibrahim_64@yahoo.com

***Abstract*—Friction welding is becoming a viable replacement of conventional joining methods. Continuous Drive Friction Welding (CDFW) is a type of friction welding used to join rods, tubes and similar shapes. Usually, the process contains a friction stage and a forging stage and the process parameters would be ticked accordingly. AA6061 is an Mg and Si aluminum alloy that is widely used in many industries. This research investigates the effect of friction time on the mechanical properties of AA6061 joints made with CDFW and the relation to the microstructure of the material and thermal profiles. It was found that AA6061 does not require a forging stage where solid joints are obtained without forging and did not fracture within the welding zones. Also, it was concluded that the process parameters are to be tailored in a way that produces a specific type of grain structure within the welding areas.**

Keywords-AA6061; continuous drive friction welding; tensile strength; yield strength; thermal profile; microstructure; time of friction

I. INTRODUCTION

Friction Welding (FW) is a form of joining materials in solid phase. Some variations of FW are Friction Stir Welding (FSW), Friction Stir Spot Welding (FSSW), and Rotational Friction Welding (RFW). Continuous Drive Friction Welding (CDFW) is a form of RFW that is used to join rods and tubes of similar and dissimilar materials. Such welding techniques allow the materials to be joined without reaching the melting temperature and prevent the formation of intermetallic layers in similar material welding. When compared to conventional welding techniques, CDFW is more favorable, less costly, and more environmentally friendly. Five process parameters are affecting CDFW: rotational speed (RS), friction pressure (P_f), friction time (t_f), upset pressure (P_u), and upset time (t_u). Some studies use burn-off length (BL) instead of t_f. In most cases, the friction time and pressure are much less than the upset time and pressure. The Upset stage is also sometimes referred to as the forging stage. Most studies consider a range of rotational speed, a variety of friction pressure, a range of upset pressure, and some specified times of friction or burn-off lengths. Most of the relevant literature is focused on the CDFW of Aluminum Alloy 6061 (AA6061) investigating specific process parameters and does not provide a complete relation of process parameters to mechanical properties, microstructure, and thermal profiles. Authors in [1] investigated the conditions of CDFW of some Al alloys. RS was set to 2000, 2500, and 2800rpm while P_f varied between 5 and 7.64Kg, P_u ranged between 17.83 and 22.93Kg, and the time of friction t_f was set to 4, 7, and 10s. The type of Al alloy was not specified, and no optimum process parameters were outlined. One of the conclusions was that the lowest speed (2000rpm) produced weak welds. The mechanical properties and microstructures for joining AA6061 with AA6082 via a conventional lathe machine were studied in [2]. The study considered a friction time of 3min and an upset pressure of 10. Friction time was too long as compared to similar studies. The tensile strength of AA6061 CDFW and the related microstructure was investigated in [3] with a constant time of friction but prolonged upset times. The highest tensile strength was achieved when the conditions were set to the highest upset pressure and time. Higher upset pressures and times correspond to higher energy and required duration for the welding procedure. On the other hand, the requirement of the prolonged upset stage was not clearly supported, and macrostructure did not provide enough evidence on the conditions of the various welding parameters.

There are some studies related to similar material welding of different Al alloys or metal matrix composites. The friction welding conditions on the mechanical properties of AA7075 and AA5052 were investigated in [4, 5]. It was concluded that the initial stage of the welding procedure as a critical factor in determining welding efficiency. A metal matrix composite consisting of AA6061 with 10wt% Al_2O_3 and SiC was studied in [6]. The considered process parameters were P_f, P_u, BL, and RS. According to the study, the best-welded samples were obtained with 2000rpm, 2mm BL, 70MPa P_f, and 130MPa P_u. It was also concluded that low BL causes weak joints where high BL causes excessive flash formations. The literature about CDFW is mainly concerned with the welding of dissimilar materials. One of the main focus areas is welding Al alloys

Corresponding author: Masoud Ibrahim Mohamed

with stainless steel as employing CDFW [7-13]. Another investigated area is joining Al with different alloys such as copper [14], plain carbon steels [15], and titanium alloys [16]. The effect of the time of friction on the mechanical properties of titanium-stainless steel welding was also investigated [17].

The process of welding similar materials via CDFW is less complicated than dissimilar material welding. However, the authors of this research paper did not come across many studies that investigate such welding conditions. Also, since materials such as Al alloys are soft and have lower melting temperatures than ferrous alloys, the requirement of a forging stage is to be questioned. The process parameters that provide excellent mechanical properties are not clearly defined, especially when it comes to the time of friction. Some studies investigated longer times while others considered shorter periods, both with upset periods. This research aims to establish the best conditions for achieving strong AA6061 joints by CDFW. Such best conditions would be investigated in terms of mechanical properties and microstructure. Finally, the necessity of the forging stage when welding such alloys is validated.

II. MATERIALS AND METHODS

AA6061 is a precipitation-hardened aluminum alloy containing Mg and Si. It has good mechanical properties and usually good weldability. The chemical composition of AA6061 in weight percentages is given in Table I. AA6061 rods (d=10 and l=65mm) were welded via CDFW process. CDFW was achieved using a conventional lathe machine. Friction and upset pressure were achieved via a hydraulic mechanism that was fabricated in the lab and attached to the lathe machine (Figure 1). The hydraulic mechanism controls and maintains the friction pressure on the fixed part side while the rotating part is fixed to the chuck of the lathe machine. The two parts to be welded are fixed on the two parts of the machine, then centered and brought together with a slight clearance left in between. The welding process starts by operating the lathe machine to start the rotating motion, and then the friction pressure is encaged and applied through the hydraulic mechanism. A timer controls the duration of the welding process and stops both rotational motion and pressure application accordingly.

TABLE I. CHEMICAL COMPOSITION OF ZL6061

Element	Si	Mg	Cu	Fe	Ti	Mn	Zn	Cr
Wt.%	0.75	0.9	0.5	0.5	0.15	0.05	0.03	0.03

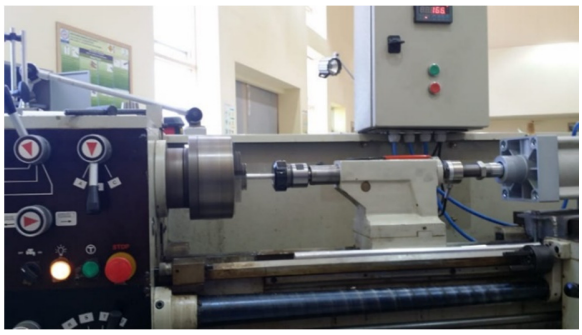

Fig. 1. Friction welding machine

The welding process was conducted according to the parameters shown in Table II. RS and P_f values were taken from [1-3, 6], which obtained good welding samples. Also, identifying the requirements of an upset stage was investigated by not including any forging in the welded samples and comparing the mechanical properties to non-welded samples. As such, the time of friction (t_f) was the only variable since it was desired to understand the effect of welding duration on the welding zones and microstructures. The lower limit was set to 4s due to the current machine capability: it was not possible to achieve welded samples in less than 4s. The welding temperature was measured using an Infrared Dual Laser Point Thermometer (operational range of -50 to 800°C, spatial accuracy of 1mm and time accuracy of 0.5s). It was calibrated to AA6061 before actual temperature measurement. The temperature measurement was video recorded and then analyzed and plotted on a PC.

TABLE II. CDFW PROCESS PARAMETERS [1-3, 6]

Parameter	Value
Rotating speed (rpm)	2000
Friction pressure (bar)	2
Friction time (s)	4, 5, 6, 7, 8, 9, 10

Five samples were acquired for each set of parameter conditions. Three samples were used for tensile testing and two were used for evaluating the welding zones and microstructure. The welded samples are shown in Figure 2. Tensile testing was carried out using a WDW-20 computer-controlled electromechanical universal tensile testing machine according to ASTM: E8 at a rate of 0.5mm/min. The samples were machined to satisfy the tensile test standards and were then tensile tested. Figure 3 shows the tensile sample dimensions. The remaining samples were cut longitudinally, using a precision cutting machine (Pico 75), ground, polished, and etched as per the requirements for such materials [3, 18]. Macroscopic graphs were obtained via a digital microscope, while microscopic micrographs were achieved by SEM.

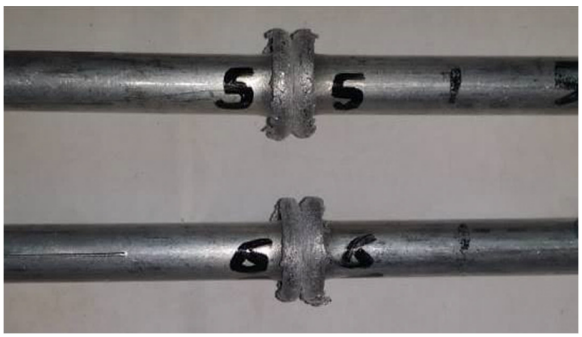

Fig. 2. Two continuous drive friction welded samples

Fig. 3. CDFW tensile sample before tensile testing

III. RESULTS

The results of the experiments include the analysis of the stress-strain curves for all welded samples as a function of friction time. The welding temperature at the interface was measured for all considered times of friction. Finally, macro and microstructure investigation were conducted.

A. Tensile Properties

The corresponding yield and tensile strength values for AA6061 were 76MPa, and 130MPa respectively. Figure 4 shows the average engineering stress-strain (σ-ε) curves as a function of the time of friction (t_f) or the welding time since no forging was involved. From Figure 4, the σ-ε curves for t_f=4, 5, and 6s seem to have relatively close σ_y and UTS values. The corresponding σ_y (0.02% ε) and UTS varied between 65 and 80MPa and between 117 and 125MPa respectively. This variation is illustrated in Figure 5. It can be shown that both σ_y and UTS do not vary much, corresponding to the friction times of 4, 5, and 6s. The samples welded at 5s had a less plastic deformation curve since each curve represents an average of three curves. One of the samples welded at 5s had poor tensile properties, hence, on average, samples welded at 5s had less plastic deformation. The other two samples welded at 5s exhibited good σ-ε curves and ductile fractures. Figure 6 shows the fracture surfaces for the samples fabricated with those friction times. Based on fracture surfaces shown in Figure 6, all samples fabricated at t_f=4, 5, and 6s (except the 5s sample mentioned earlier) fractured in a ductile manner, and the fracture occurred within the base metal outside of the welding zones.

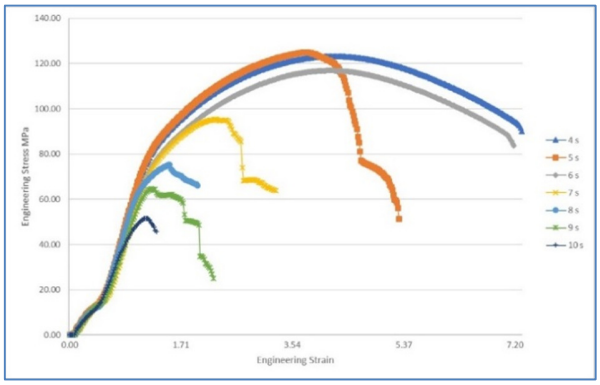

Fig. 4. Engineering stress vs engineering atrain (average) as a function of friction time

On the other hand, the σ-ε curves for the higher friction or welding time, i.e., t_f equal to 7, 8, 9, and 10s show different indications. It can be seen from Figure 5 that σ_y and UTS for these welding times are much less than the short-time welded samples. σ_y and UTS for the CDFW sample at t_f=7s were 69MPa and 103MPa respectively on average with a substantial variation in UTS between 124 and 86MPa. The large variation in UTS was because one sample exhibited ductile failure, and the failure location was outside the welded area, while the other two samples exhibited brittle failure that was initiated from the interface between the welded surfaces as shown in Figure 6. All the remaining samples for welding times 8, 9, and 10s failed in a brittle manner, hence the deficient tensile properties shown in Figures 4 and 5. When the friction time was set to 8s, σ_y and UTS values were found to be about 55MPa and 83MPa, respectively (on average). A large variation in UTS was observed, as indicated in Figure 5. The variation in UTS, in this case, was because two samples failed at the interface with very little material mixing (similar to the failure surfaces shown in Figure 7), while one sample failure showed signs of moderate material joining as shown in Figure 6. As the friction time increased to 9s, σ_y and UTS were measured at 57 and 73MPa, respectively (on average) with a little variation in UTS. Finally, σ_y and UTS were measured at 47 and 57MPa, respectively (on average) when the welding time was set to 10s. All welded samples fabricated at 9 and 10s failed at the welding interface with very little material mixing, as shown in Figure 8.

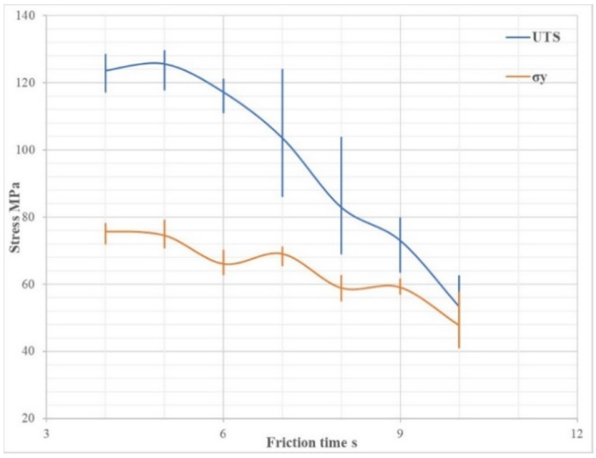

Fig. 5. Average tensile strength and yield strength of Al6061 CDFW samples as a function of welding time

TABLE III. MAIN MECHANICAL CHARACTERISTICS RETAINED FROM THE STRESS-STRAIN CURVES

Welding time (s)	Yield strength (MPa)	UTS (MPa)
4	76	124
5	74	126
6	66	117
7	68	104
8	58	83
9	59	73
10	48	54

B. Thermal Profiles

The thermal profile of the welding procedure during CDFW was investigated by recording the welding temperature during the welding procedure. Figure 9 shows the variation of temperature as a function of time for the various welding times considered in this work. The data were used for constructing the temperature curves of the average of the three measurements at each welding time. Temperature change per second was video-recorded during the experiments. The maximum average temperature (highest peak) seems to be relatively close for all samples except for the sample welded at 10s. Also, the average peak temperature for all samples occurred between 3 and 4s, as shown in Figure 9. The average maximum temperature (welding times: 4-9s) varied between 175 and 185°C while it was 152°C for samples welded at 10s.

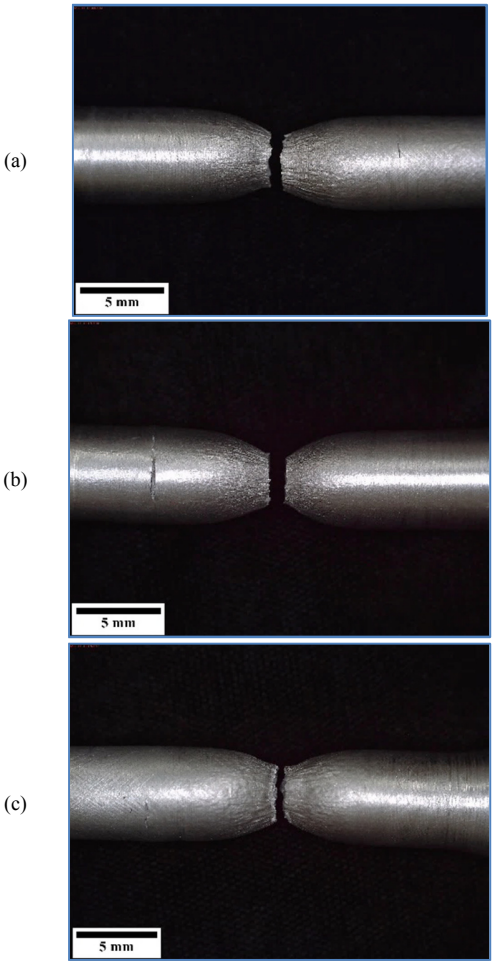

Fig. 6. Fracture surfaces for t_f: (a) 4s, (b) 5s, (c) 6s

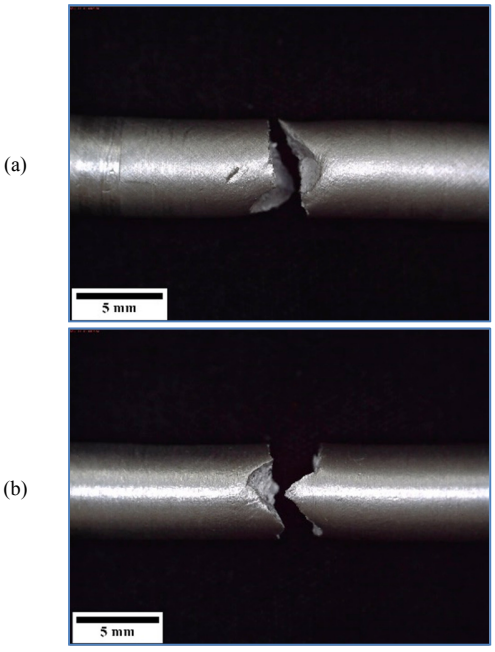

Fig. 7. Fracture surfaces for t_f: (a)7s, (b) 8s

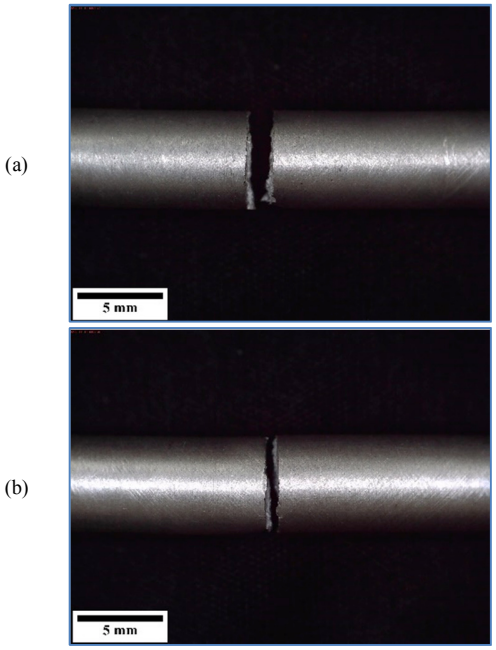

Fig. 8. Fracture surfaces for t_f=: (a) 9s, (b) 10s

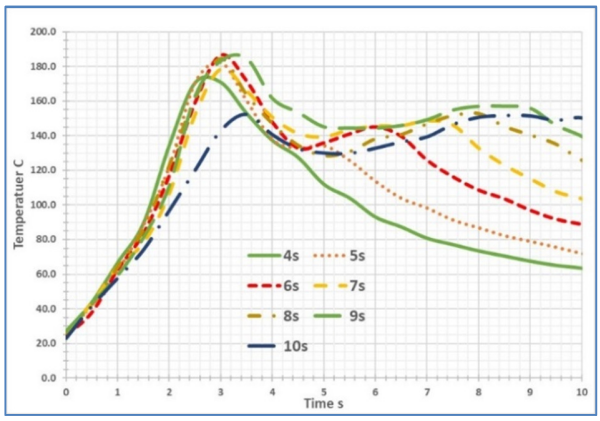

Fig. 9. Average welding temperature as a function of time for CDFW Al6061 rods

Meanwhile, the cooling curves for higher friction times seemed to decrease for 2-3 seconds, increase again to a temperature lower than the maximum temperature obtained before, and then continuously decrease until reaching room temperature. The profiles of the thermal curves shown in Figure 9 indicate that a friction time of 4s may be adequate for welding AA6061 samples (with the considered process parameters). Any further increase in welding time affects slightly the maximum temperature but causes a second increase in temperature that might be critical on the mechanical properties of the welded joint.

C. Microscopy

The welded joints were investigated further with a digital microscope and SEM. Figure 10 represents the longitudinal cross-sections of welded samples at different welding times. The 4 and 6s illustrations on top represent the samples that exhibited reliable welding while the 7 and 8s illustrations on

the bottom represent the samples that showed poor welding. Another justification for this analogy is the fact that σ-ε curves for both 4 and 6s provided optimistic tensile properties while the σ-ε curves for 7 and 8s exhibited poor tensile properties.

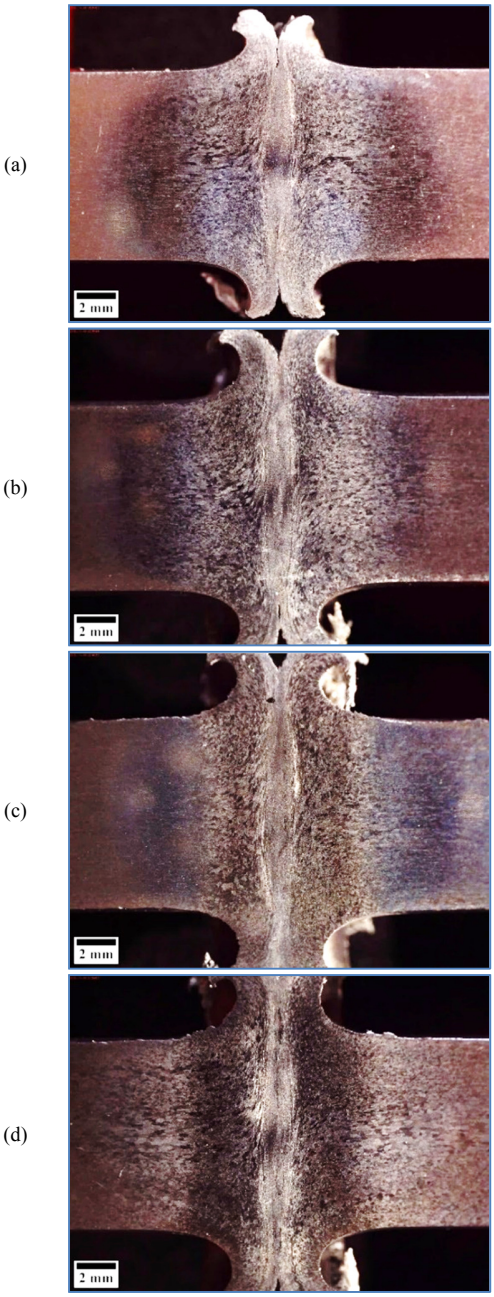

Fig. 10. Longitudinal cross-sectional view of the welds at (a) 4s, (b) 6s, (c) 7s, (d) 8s

The samples welded at t_f equal to 9 or 10s were not considered anymore since such welding times produce inferior welds for CDFW AA6061 as shown earlier. Referring to the illustrations shown in Figure 10, the sample welded at 4s exhibited minimal flash and the total thermally affected area seems to be relatively large. On the other hand, the 8s welded sample exhibited a large flash, a less total thermal affected area, and a dark region surrounding the welded area inductive of undergoing higher thermal cycles. The samples welded at 6, and 7s fall between the conditions for the 4, and 8s welded samples. In these samples, the total thermally affected area starts decreasing, and the formation of the dark area surrounding the welding area starts becoming visible. Lastly, the width of the central part of the welded area seems to be similar across all samples. To compare the microstructures of the welded samples shown in Figure 10, zoomed images were obtained with the digital microscope as shown in Figure 11 and SEM micrographs, as shown in Figure 12.

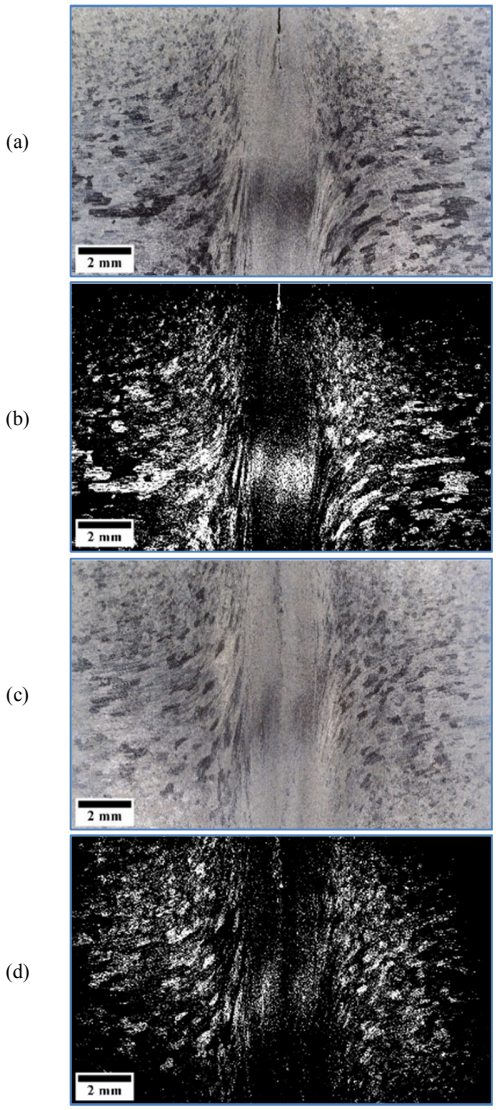

Fig. 11. Comparing the macrostructure among welding times of 4s (upper two images), and 8s (lower two images)

In order to highlight the effect of welding time on microstructure, the welding times of 4 and 8s were selected. ImageJ was used to further analyze these images by reducing them to black and white, as shown in Figure 11. The 4s welded sample seemed to have a combination of large and small grains

while the 8s sample seemed to have almost uniform grain size. The grain size distribution appears to become more consistent as welding time increases. Another observation from Figure 11 is that shorter welding times seem to produce finer grains in the near-flash area (upper areas) as compared to longer welding times. The grain size distribution for the 4s welded sample seems to increase gradually from the near-flash area to the center. Such a feature is not distinctive for the 8s welded sample shown on the bottom right illustration in Figure 11. Scanning Electron Microscopy was performed on 4s and 8s welded samples to further investigate the evidence of microstructure differences. Figure 12 shows the SEM micrographs for the welded samples at 4s (upper), and 8s (lower). We can see that there is a clear difference in the microstructure and comparing the SEM micrographs outlines some of these differences. The grains at 8s welding time were almost the same sizes and grown to relatively uniform sizes, while the 4s sample had a range of non-uniformly sized grains. Furthermore, the 4s welded sample showed many tiny white particles that could be inductive of nucleation of new grains while the 8s welded sample has no such feature.

(a)

(b)

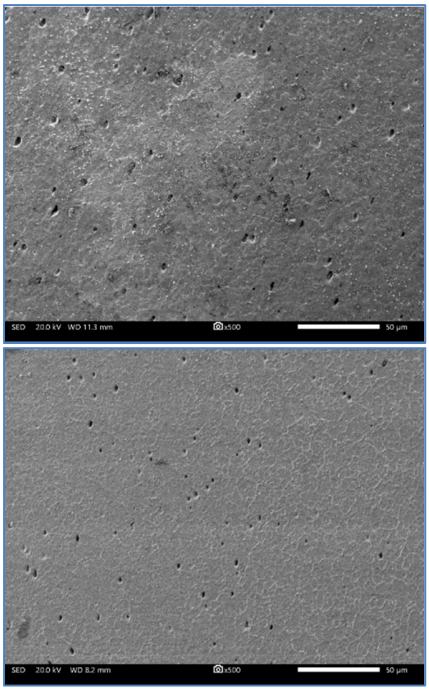

Fig. 12. SEM micrographs of the microstructure of samples welded at (a) 4s, (b) 8s

IV. DISCUSSION

CDFW of AA6061 seems to depend on the condition of the resulting microstructure. The process parameters considered in this study are shared among the studies related to CDFW of AA6061, yet the results about thermal cycles and short welding times are innovative. Samples welded with less than 6s of friction time without any upset had superior tensile properties than samples welded at longer welding times with similar conditions. The tensile properties of the welded joint decrease significantly as welding time increases, as shown in Figures 4 and 5. Such decline is directly related to the microstructure resulting in each case and the thermal cycles exerted on the joint. With shorter friction time, the material had just enough time to initiate plastic deformation, start mixing with the material from the other side, and form new grain nucleation sites within the original grains. Such effect was demonstrated as tiny white dots, and large grains within the same structure for the sample welded at 4s. As the welding time increases, more material is mixed, and the new nucleating grains had enough time to grow, become fully developed, and have uniform grain size distribution. On average, the 5s welded sample had less plastic deformation than the 4 and 6s welded samples. Such a phenomenon can be attributed to just a weak welding sample that provided this result. Nevertheless, the samples welded at 4s without a doubt were the best in terms of tensile properties. As the welding time increases beyond 6s, the properties become unstable. The samples welded at 7 and 8s showed mixed indications. One of the 7s samples failed in a ductile manner, while the other two failed in a brittle way. Two of the 8s samples failed in a brittle way with evidence of some material joining while one failed in a simple brittle manner with little or no material joining. Such effects become even more distinctive for the 9s and 10s where all samples failed within the welding surface in a brittle way with almost no material joining. The thermal profiles can be related to such phenomena.

The maximum welding temperature occurs around 3-4s in all cases and reaches more than 180°C in most. The thermal profile during CDFW was investigated in [15, 21-23]. Most of the research efforts related to thermal profiles are about finite element analysis modeling and about connecting the thermal profile during the process in both experiments and models. The research related to thermal effects on the microstructure is almost none, especially for the considered material. Also, most of the thermal modeling research observed show only one peak of temperature and never two peaks. Any increase of welding time beyond 4s results in a gradual rise in the heat generated within the welding area, causing no additional material joining but acting like a thermal cycle which develops the grain structure. Grain structure seems to become fully developed at higher welding times resulting in weak tensile properties, as shown Figures 4 and 5. The microstructure illustrations support this claim, indicating more uniform grain structure at longer welding times and the development of the dark areas surrounding the welded area, indicating higher thermal cycles. The best welding conditions are when the process parameters are such that the material has just enough time for mixing and initiating new grains. Any process parameter combination that leads to fully developed grains and extended thermal cycles is not favorable and can flaw welding properties. The non-uniform grain size distribution obtained with lower welding times seems to affect the plasticity by introducing more grain boundaries and dislocations hence preventing the advancement of any cracks or defects within the welded area. Such a result appears to be logical since all samples welded at 4-6s (except for one-sample welded at 5s) failed within the base metal away from the welded areas. Also, less welding time indicates less material consumption, less energy required for welding, and, therefore, less operational cost.

V. CONCLUSION

The effects of the process parameters of CDFW, especially the time of friction on the mechanical, thermal, and structural properties of AA6061 were investigated. The tensile tests indicated that no forging is required when joining such alloys with CDFW and that a short time of friction would result in strong joints. On the other hand, the thermal profiles of the welding times indicated that the peak temperature is reached within 3 to 4s of the welding process regardless of the duration of the welding procedure. Any further increase in the time of friction does not increase the temperature beyond the peak temperature obtained earlier but helps annealing the material. Macro and micro structure investigations showed that the process parameters should be handled in a way to produce a mixture of grain sizes and not allow the grains to fully develop and grow in size. The more uniform the grain size of the welding area, the weaker the welding joint.

ACKNOWLEDGMENT

The authors acknowledge the funding of the Deanship of Scientific Research at Northern Border University, according to the research grant No. ENG-2018-3-9-F-7724. Also, the authors acknowledge the assistance provided by Dr Nidhal Beshiekh and Dr Mohamad Gameel in performing some of the experimental procedures specified in this paper.

REFERENCES

[1] B. S. Yilbas, A. Z. Sahin, A. Coban, B. J. Abdul Aleem, "Investigation into the properties of friction: welded aluminium bars", Journal of Materials Processing Technology, Vol. 54, pp. 76–81, 1995

[2] J. Tijo, K. Vinoj, "Friction welding of Aluminium 6061 and Aluminium 6082 rods by using conventional lathe", International Journal of Current Trends in Engineering & Research, Vol. 2, No. 4, pp. 170-175, 2016

[3] F. A. M. Abdulla, Y. S. Irawan, D. B. Darmadi, "Tensile strength and macro-microstructures of A6061 CDFW weld joint influenced by pressure and holding time in the upset stage", Jurnal Rekayasa Mesin, Vol. 9, No. 2, pp. 149–154, 2018

[4] M. Kimura, M. Choji, M. Kusaka, K. Seo, A. Fuji, "Effect of friction welding conditions on mechanical properties of A5052 aluminium alloy friction welded joint", Science & Technology of Welding & Joining, Vol. 11, No. 2, pp. 209–215, 2006

[5] M. Kimura, M. Choji, M. Kusaka, K. Seo, A. Fuji, "Effect of friction welding conditions and aging treatment on mechanical properties of A7075-T6 aluminum alloy friction joint", Science & Technology of Welding & Joining, Vol. 10, No. 4, pp. 406–412, 2005

[6] R. Adalarasan, M. Santhanakumar, A. S. Sundaram, "Investigation in solid-state joining of Al/SiC/Al2O3 composite using Grey-based desirability (GBD) and response surface plots", Journal of the Chinese Institute of Engineers, Vol. 40, No.1, pp. 55–65, 2017

[7] M. Sahin, "Joining of stainless-steel and aluminium materials by friction welding", International Journal of Advanced Manufacturing Technology, Vol. 41, pp. 487–497, 2009

[8] P. Sammaiah, A. Suresh, G. R. N. Tagore, "Mechanical properties of friction welded 6063 aluminum alloy and austenitic stainless steel", Journal of Material Science, Vol. 45, pp. 5512–5521, 2010

[9] M. G. Reddy, S. A. Rao, T. Mohandas, "Role of electroplated interlayer in continuous drive friction welding of AA6061 to AISI 304 dissimilar metals", Science & Technology of Welding & Joining, Vol. 13, No. 7, pp. 619–628, 2008

[10] S. D. Meshram, G. M. Reddy, "Friction welding of AA6061 to AISI 4340 using silver interlayer", Defence Technology, Vol. 11, No. 3, pp. 292–298, 2015

[11] Z. Liang, G. Qin, P. Geng, F. Yang, X. Meng, "Continuous drive friction welding of 5A33 Al alloy to AZ31B Mg alloy, Journal of Manufacturing Processes, Vol. 25, pp. 153–162, 2017

[12] S. Celik, D. Gunes, "Continuous drive friction welding of Al/SiC composite and AISI 1030", Welding Journal, Vol. 91, pp. 222S–228S, 2012

[13] E. P. Alves, F. Piorino Neto, C. Y. An, "Welding of AA1050 aluminum with AISI 304 stainless steel by rotary friction welding process", Journal of Aerospace Technology and Management, Vol. 2, No. 3, pp. 301–306, 2010

[14] M. Sahin, "Joining of aluminium and copper materials with friction welding", International Journal of Advanced Manufacturing Technology, Vol. 49, No. 5-8, pp. 527–534, 2010

[15] T. C. Nguyen, D. C. Weckman, "A thermal and microstructure evolution model of direct-drive friction welding of plain carbon steel", Metallurgical and Materials Transactions B, Vol. 37, No. 2, pp. 275–292, 2006

[16] M. A. Tashkandi, J. A. Al-jarrah, M. Ibrahim, "Spot welding of 6061 Aluminum alloy by friction stir spot welding process", Engineering Technology & Applied Science Research, Vol. 7, No. 3, pp. 1629-1632, 2017

[17] J. A. Al-jarrah, A. Ibrahim, S. Sawlaha, "Effect of applied pressure on mechanical properties of 6061 Aluminum alloy welded joints prepared by friction stir welding", Engineering, Technology & Applied Science Research, Vol. 7, No. 3, pp. 1619-1622, 2017

[18] M. Avinash, G. V. Chaitanya, D. K. Giri, S. Upadhya, B. K. Muralidhara, "Microstructure and mechanical behaviuor of rotary friction welded titanium alloys", International Journal of Mechanical, Industrial and Aerospace Sciences, Vol. 1, No. 11, 2007

[19] P. Li, J. Li, M. Salman, L. Liang, J. Xiong, F. Zhang, "Effect of friction time on mechanical and metallurgical properties of continuous drive friction welded Ti6Al4V/SUS321 joints", Materials & Design, Vol. 56, pp. 649–656, 2014

[20] C. J. Smithells, W. F. Gale, T. C. Totemeier, Smithells metals reference book, Elsevier, 2003

[21] A. B. Dawood, S. I. Butt, G. Hussain, M. A. Siddiqui, A. Maqsood, F. Zhang, "Thermal model of rotary friction welding for similar and dissimilar metals, Metals, Vol. 7, Article ID 224, 2017

[22] E. Bouarroudj, S. Chikh, S. Abdi, D. Miroud, "Thermal analysis during a rotational friction welding", Applied Thermal Engineering, Vol. 110, pp. 1543–1553, 2017

[23] A. Can, M. Sahin, M. Kucuk, "Modeling of friction welding, International Scientific Conference, Gabrovo, Bulgaria, November 19-20, 2010

AUTHORS PROFILE

Mohammed A. Tashkandi is an associate professor in the Mechanical Engineering Department at Northern Border University in Saudi Arabia. He graduated from Colorado State University, Fort Collins, Co. His research interests include material engineering, various methods of friction welding such as stir friction welding, stir spot friction welding and continuous drive friction welding. He is also familiar with design of experiments, optical microscopy, and scanning electron microscopy.

Masoud Ibrahim Mohamed is a professor of Materials Science on leave from the Mechanical Engineering Department at Fayoum University, Egypt. He is currently working in the Chemical Engineering at Northern Border University, Saudi Arabia. His research interests include material science of ferrous alloys and some light alloys such as aluminum and copper alloys. He is interested explicitly in phase analysis of different materials corresponding to different conditions and the relation to the mechanical properties of such materials.